

THE EFFECT OF GLOBAL-SCALE DIVERGENT CIRCULATION ON THE ATMOSPHERIC WATER VAPOR TRANSPORT AND MAINTENANCE, Tsing-Chang Chen, Department of Earth Sciences, Iowa State University, Ames, IA 50011

1. Introduction

Many efforts have been made by meteorologists in the past three decades to examine the local maintenance of water vapor by the moisture transport. It was pointed out by Starr and Peixoto (1) that it is difficult to explain the relationship between regions of high water vapor content and total moisture. As it is well known, the precipitation caused by condensation is often associated with the vertical motion of atmospheric divergent circulation. Based upon this practice, we would like to show how the high water vapor content over certain regions is attributed to the convergence by divergent circulations. Two aspects will be presented. One aspect is how the high water vapor content in the tropics during winter and summer seasons is maintained. The other is how the sudden intensification of the tropical divergent circulations associated with the monsoon onset enhances the water vapor content over monsoon regions. The data used in this study were generated by the FGGE III-b analyses of the European Center for Medium Range Weather Forecasts. The specific humidity is computed from temperature and relative humidity in Chen et al. (2).

2. Theoretical Background

The hydrological cycle of the atmosphere can be illustrated with the water balance equation,

$$\frac{\partial W}{\partial t} + \nabla \cdot \mathbf{Q} = E - P, \quad (1)$$

where W is precipitable water in an air column, \mathbf{Q} is water vapor transport, ∇q , and q is specific humidity. E and P are evaporation and precipitation. The long-term, say a season or a month, average of Eq. (1) can be approximated as

$$\nabla \cdot \bar{\mathbf{Q}} = \bar{E} - \bar{P}, \quad (2)$$

($\bar{\quad}$) = time average. Note that the water vapor transport vector can be separated into the rotational and divergent component, i.e. $\nabla q = (\nabla q)_\psi + (\nabla q)_\chi$ or $Q = Q_\psi + Q_\chi$. These two components can be expressed in terms of streamfunction (ψ) and potential function (χ). Therefore, Eq. (2) can be written as

$$\nabla \cdot \bar{\mathbf{Q}}_\chi = \nabla^2 \bar{\chi} = \bar{E} - \bar{P}. \quad (3)$$

Based upon Eq. (3), we can relate \mathbf{Q} to the source and sink of water vapor. This approach was proposed by Chen χ (3). ψ and χ are obtained from Poisson equation by specifying boundary conditions at the northern and southern boundaries. Our analysis covers the entire globe.

3. Global Water Vapor Flux and Maintenance

The largest water vapor content exists in the tropics. The zonal asymmetry in the geographic distribution of this quantity occurs essentially over three tropical continents. They are the northern part of South America,

equatorial Africa, and the equatorial western Pacific during the northern winter (December-February), and Central America and the northern part of South America, equatorial west Africa, and monsoon areas during the northern summer (June-August). The water vapor transport is mainly carried out by Q_{ψ} (not shown) and follows the low-level atmospheric circulations because the major part of the water vapor is located there. According to Eq. (2), Q_{ψ} is not related to the difference between evaporation (E) and precipitation (P), while Q_{χ} is. The latter component of water vapor transport is displayed in Fig. 1 for both northern summer and winter. Observations reveal that the water vapor converges toward three tropical areas of high water vapor content. This indicates that the local Hadley circulation and the longitudinal Walker circulation perform the water vapor transport to maintain the high water vapor content over three preferable tropical regions. The converged water vapor would be transported upward by the two types of divergent circulations to increase the moisture content of the atmosphere and, in turn, to enhance the condensation. Therefore, the large rainfall in the tropics is consistently distributed with the significant convergence of water vapor flux.

4. Divergent Water Vapor Flux Associated with Monsoon Onset

The onset of both Australian and Indian monsoon is always characterized by the deepening of the low-level monsoon trough and the intensification of the upper-level high center over monsoon regions, and sudden heavy rainfall (Chen and Yen (4)). This implies the abrupt development of divergent circulations over monsoon regions when the monsoon onset occurs. The strong upward motions associated with divergent circulations converge and pump upward water vapor. Intensive cumulus convective activities are induced and heavy rainfall follows. The moisture transported by the divergent mode before and after monsoon onset for both Australian and Indian monsoon is exhibited in Figs. 2 and 4, respectively. The onset of the former monsoon occurs between December 21-26 of 1978 and that of the latter monsoon occurs between June 10-16, 1979. It is very obvious from these two figures that a tremendous enhancement of water vapor flux converged toward monsoon regions by the divergent mode after monsoon onset occurs. To demonstrate the abrupt increase of water vapor with divergent circulations when the monsoon onset occurs, averages of the 200-mb divergent kinetic energy (k_D), water vapor content, and root mean square of divergent water vapor flux over key monsoon areas, which are encircled in Figs. 2 and 4, are displayed in Figs. 3 and 5. These figures confirm our above argument.

5. Concluding Remarks

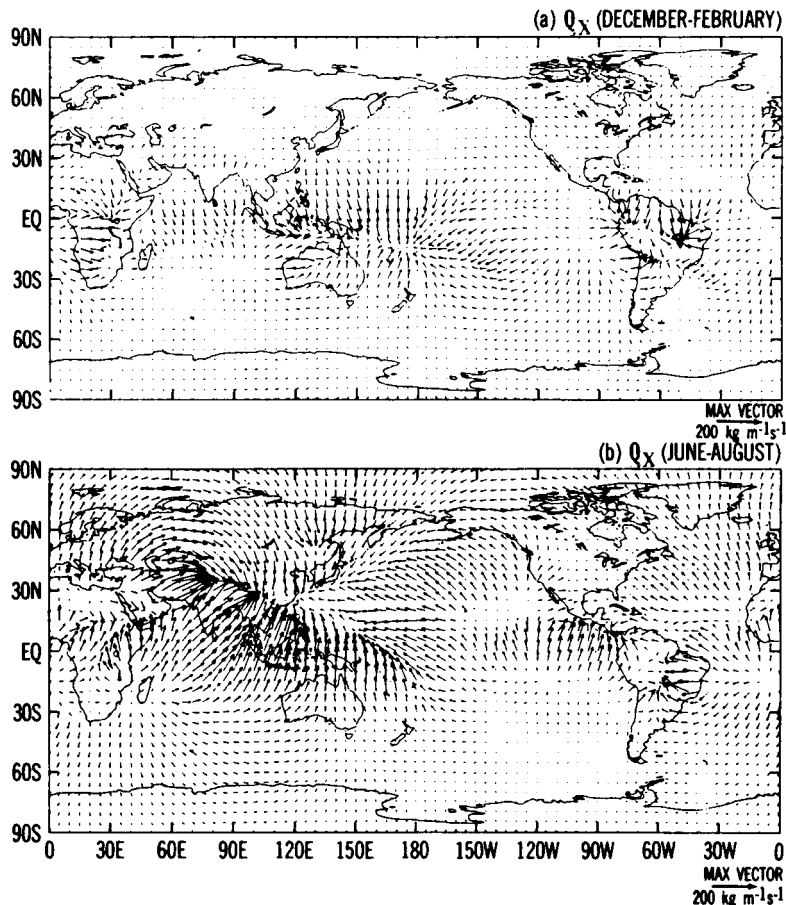
It was shown by our past studies (Chen and Wiin-Nielsen (5); Chen (6)) that the atmospheric circulation is dominated by the rotational component. However, it is the divergent component of motion which releases the available potential energy to drive atmospheric motions. The water vapor transport by atmospheric motions works in a same manner. Although the water vapor is essentially transported by rotational component, this study demonstrates that only the water vapor transported by divergent component is linked to the source and sink, and maintenance of atmospheric water vapor content.

6. Acknowledgements

This study is supported by the NSF Grant ATM-8611476. Figs. 2-5 were prepared by Mr. M.-C. Yen, whose help is highly appreciated. The computations were performed with the NCAR CRAY computer which is sponsored by the National Science Foundation. Thanks also go to Ms. Linda Claussen for her typing.

7. References

- Starr, V. P. and Peixoto, J. P. (1964), Arch. Meteor. Geoph. Biokl., Ser. A, 14, p. 111-130.
- Chen, T.-C., Chang, C. B., and Perkey, D. J. (1985), Monthly Weather Review 113, p. 349-361.
- Chen, T.-C. (1985), Monthly Weather Review, 113, p. 1801-1819.
- Chen, T.-C. and Yen, M.-C. (1986), The Second International Conference on Southern Hemisphere Meteorology, 1-5 December 1986, Wellington, New Zealand.
- Chen, T.-C. and Wiin-Nielsen, A. (1976), Tellus, 28, 486-498.
- Chen, T.-C. (1980), Monthly Weather Review, 108, p. 896-912.

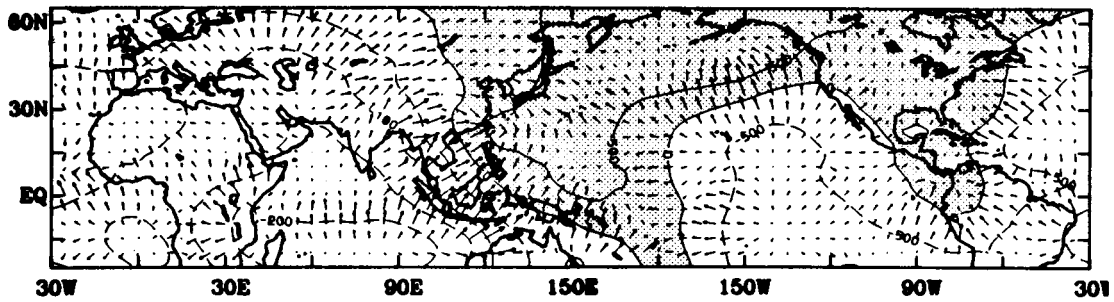


ORIGINAL PAGE IS
OF POOR QUALITY

Fig. 1. Divergent component of the vertically integrated water vapor transport vector field. Vector units: $\text{kg m}^{-1}\text{s}^{-1}$.

Q_D and χ

(a) 5/20-6/2 (1979) before onset of Indian monsoon



(b) 6/17-6/30 (1979) after onset of Indian monsoon

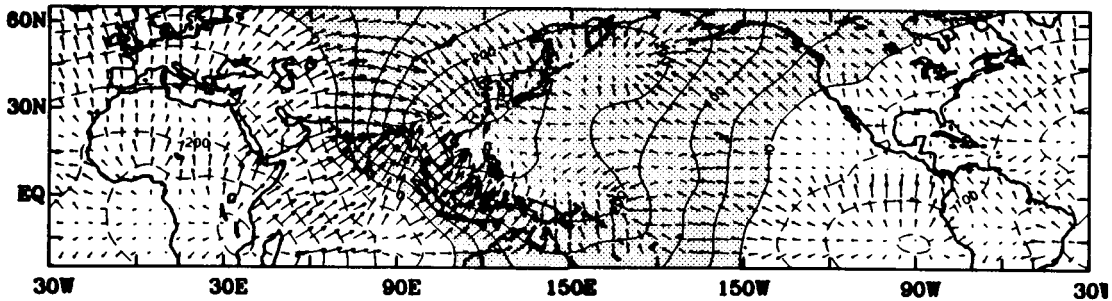


Fig. 2. Global distribution of potential for the vertically integrated water vapor flux superimposed with divergent component of water vapor transport vector field. Contour intervals of potential are 5×10^5 kg s^{-1} and vector units are $\text{kg m}^{-1} \text{s}^{-1}$.

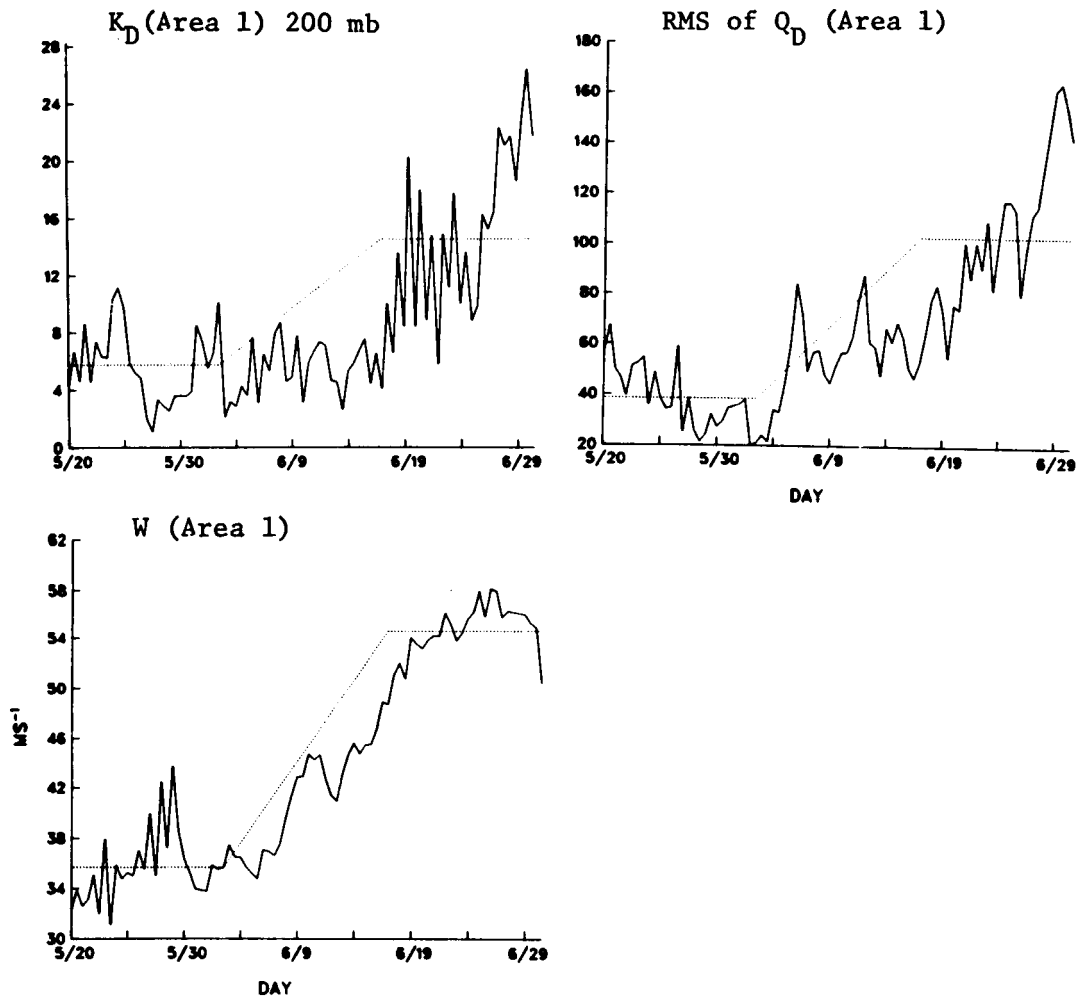
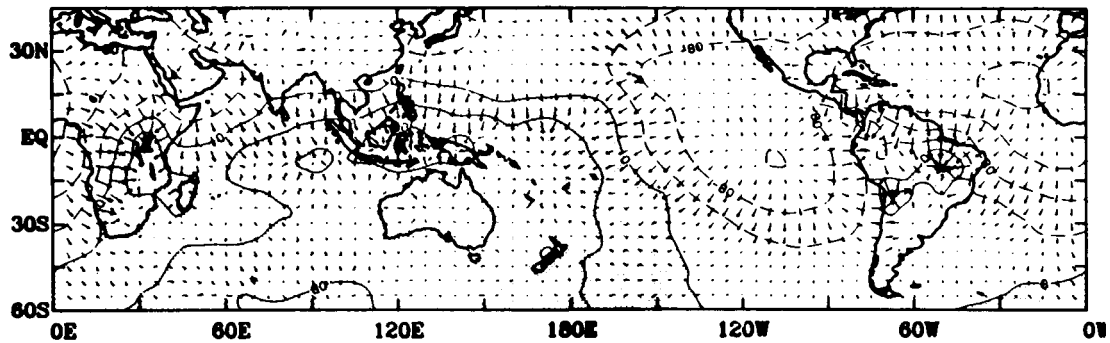


Fig. 3. Time series of K_D , root mean square (RMS) of Q_D and precipitable water (W). Area 1: ($60^{\circ}E-90^{\circ}E$, $15^{\circ}N-25^{\circ}N$)
 Units: K_D m^2s^{-2} , RMS of Q_D $ms^{-1}g\ kg^{-1}$,
 W mm.

Q and χ

(a) 12/1-12/21 (1978) before onset of Australian monsoon



(b) 1/1-1/31 (1979) after onset of Australian monsoon

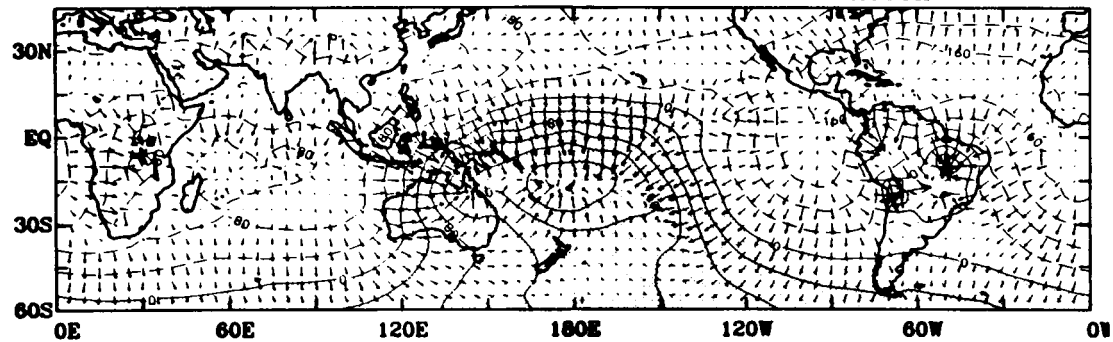


Fig. 4. The same as Fig. 2, except for the onset of Australian monsoon. Contour intervals of potential are 4×10^5 .

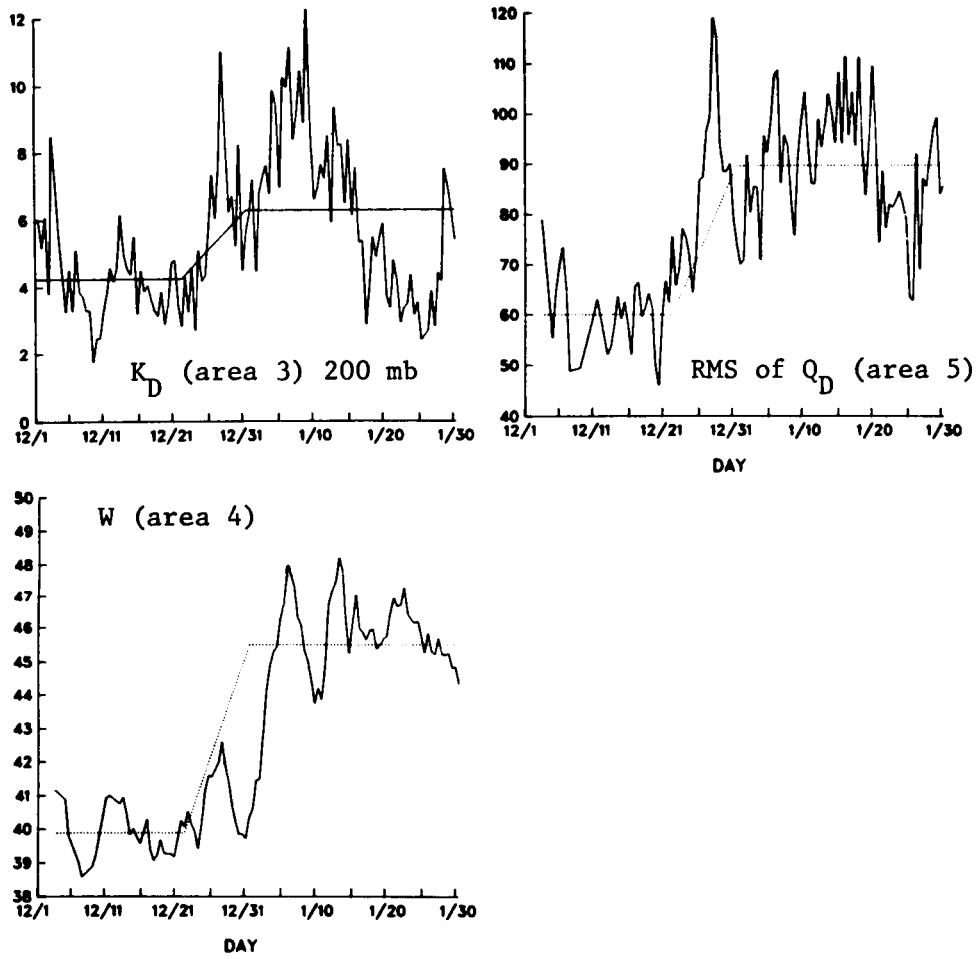


Fig. 5. Time series of K_D , root mean square (RMS) of Q_D and precipitable water (W).

Area 3: (112.5°E-120°W, 45°S-10°S)

Area 4: (150°E-140°W, 20°S-5°S)

Area 5: (112.5°E-150°W, 30°S-0°)